# Extraction of higher twists from electron-proton inclusive data at large Bjorken $x$

I. Niculescu,[2] C. Keppel,[1,2] S. Liuti,[3,4] and G. Niculescu[2]
[1]*Thomas Jefferson National Accelerator Facility, 12000 Jefferson Avenue, Newport News, Virginia 23606*
[2]*Hampton University, Hampton, Virginia 23668*
[3]*Institute of Nuclear and Particle Physics, University of Virginia, Charlottesville, Virginia 22901*
[4]*INFN, Sezione Sanità, Physics Laboratory, Istituto Superiore di Sanità, Viale Regina Elena, 299, I-00161 Rome, Italy*
(Received 7 August 1998; revised manuscript received 12 March 1999; published 14 September 1999)

We extract the power corrections to the ''scaling'' proton structure function $F_2(x,Q^2)$ by using QCD moments obtained from the world's inclusive lepton-proton scattering data. As opposed to previous analyses, we take particular account of data at large Bjorken $x(x>0.75)$ which are dominated by nucleon resonances and which make up most of the structure function at low $Q^2(Q^2 \leqslant 4\ \mathrm{GeV}^2)$. We discuss possible improvements on the determination of the magnitude of the higher twist coefficients that could be obtained from a new set of measurements of the nucleon structure functions at large $x$ and moderate $Q^2$. [S0556-2821(99)07913-8]

PACS number(s): 13.60.Hb

## I. INTRODUCTION

In this paper, we address the question of the extraction of parton distributions and higher twist[1] effects from lepton-proton scattering at large Bjorken $x$. Here $x=Q^2/2M\nu$, $Q^2$ is the four-momentum transfer, $M$ is the nucleon mass, and $\nu$ is the energy transfer. This question can now be investigated in more detail than in previous analyses both because of the abundance and precision of the experimental data at low $Q^2(0.5\ \mathrm{GeV}^2 \leqslant Q^2 \leqslant 10\ \mathrm{GeV}^2)$ recently obtained at SLAC [1,2] and at Jefferson Lab [3], and because of the accessibility of a much wider $Q^2$ regime ($Q^2$ up to $4\times10^4\ \mathrm{GeV}^2$) at the DEJY electron-proton collider HERA [4]. It is now possible to determine accurately the $Q^2$ dependence of the proton structure function at large $x$ in a wide interval of $Q^2$, thereby enabling a quantitative comparison with the predictions of perturbative QCD (PQCD).

As opposed to the lower $x$ kinematic regions which have provided the grounds for earlier accurate tests of PQCD (for reviews see, e.g., [5,6]), large $x$ physics is characterized by the fact that, for probes with $Q^2$ of a few $\mathrm{GeV}^2$, the invariant mass, $W$, of the final hadronic system is small ($W \to M$). Therefore, nonperturbative effects are expected to dominate the cross section. The kinematics of [1–3] correspond to the region of low $W$. In terms of the kinematic variables introduced above, $W=\sqrt{M^2+Q^2(1/x-1)}$ ranges from the elastic ($W \approx M$) to just overlapping the deep inelastic (DI, $W \geqslant 2$ GeV) region. Only recently have large $x$ experimental data [4] at the high end of the $W$ and $Q^2$ spectrum, i.e, far into the DI region, been available.

These latter data have been at the center of an intense debate about the possibility of detecting physics beyond the standard model. As was initially pointed out in [7,8], the definition of what is ''within the standard model'' strictly depends on the choice of the *input* parton distributions employed in the QCD evolution equations which give predictions at the values of $Q^2$ of interest ($Q^2 \geqslant 10^4\ \mathrm{GeV}^2$) to the debate. In other words, a more detailed knowledge of the structure functions at large $x$, but low $Q^2$ is needed in order to ensure unambiguous tests of this potential physics beyond the standard model.

Current parametrizations are constrained very little by inclusive data at large $x$, (see, e.g., [9] and [10]), the main reason being that the analyses of such data run into potential pitfalls implicit in the handling of nonperturbative effects (i.e., the resonance spectra). The question that naturally arises is: is it possible to establish an unbiased constraint by direct examination of the low $Q^2$, high $x$ proton structure functions? A first answer has been proposed by and Bosted Rock in Ref. [8]. However, the behavior of the parton distributions that they suggest for high $x$ assumes *duality* (discussed below) to hold in this kinematic region where it need not necessarily [11] due to higher twist contributions.

The approach that we develop here for the analysis of the proton structure function in the resonance-dominated large $x$ region is aimed at disentangling the contribution of power corrections up to the first few coefficients of the twist expansion in order to determine accurately the detailed $Q^2$ and $x$ dependence of the $F_2$ structure function at large $x$.

A long debate began over two decades ago regarding the interpretation of the resonance region and its possible connection with the DI data. In an initial phase, a number of papers were devoted to extending *duality* ideas, which successfully explained hadron-hadron scattering [12], to electroproduction [13]. Bloom and Gilman [13] showed that it was possible to write a finite energy sum rule (FESR) for the electron-nucleon structure functions. The FESR equates the integral over $\nu$ of the structure function $\nu W_2(\nu,Q^2)$, evaluated in the resonance region (i.e., at some ''low'' $Q^2$), to the integral over a scaling variable, $\omega'$, of the same structure function in the DI region (i.e., at some ''high'' value of $Q^2$). The resonance structure function $\nu W_2(\nu,Q^2)$, which approaches $F_2(x)$ or $F_2(\omega')$ in the scaling limit, was predicted to be equivalent in average to the DI one, provided the averages were taken over the same interval in $\omega'$. Bloom and Gilman's duality explained rather successfully the data in the

[1]We use here the term *twist*, $\tau$, according to its rigorous definition in QCD $\tau$=(dimension)-(spin), at variance with a quite commonly used meaning of spurious $Q^2$ dependence of nonperturbative origin.

 ©1999 The American Physical Society

range 1 $\mathrm{GeV}^2 \leqslant Q^2 \leqslant 10\ \mathrm{GeV}^2$.

The Bloom-Gilman duality picture found a natural explanation within QCD, where predictions of the high $Q^2$ behavior of the nucleon structure functions from their low $Q^2$ values are understood in terms of QCD evolution [5,6]. An analysis of the resonance region within QCD was first presented in [14] where Bloom and Gilman's approach was critically reinterpreted [14]: the integrals in the FESR were replaced by the moments of the structure functions and the fall of the resonances along a background curve with increasing $Q^2$ was explained in terms of the QCD twist expansion of the structure functions. The conclusion of Ref. [14] was that duality is equivalent to the statement that the moments of the full proton structure function at some finite (low) $Q^2$ are equal to the moments of the scaling[2] part of the structure function, differing only by $O(1/Q^2)$ or higher inverse power violations coming from the twist expansion. In this interpretation, duality persists as long as these violations are small or, as we will explain in more detail later, as long as one calculates the moments at large enough values of $Q^2$ and not exceedingly high ''$n$'' ($n$ being the conjugate variable in the Mellin transform).

Our study of higher twist coefficients by including the resonance region contribution to the QCD moments is consistent with the approach introduced in [14] (see also more recent papers, e.g., [11]) in that it is equivalent to looking for violations to Bloom-Gilman (BG) duality in the region where these violations are expected to be small. A fundamental point is that our analysis includes PQCD corrections quantitatively, making use of the newly available wide and accurate set of data in the region $x > 0.75$ and $Q^2 \lesssim 20\ \mathrm{GeV}^2$ [1,2]. Our analysis should be viewed as an initial feasibility study for an extracting higher twist corrections using QCD moments. This study differs from current analyses performed directly in $x$ space [15] with kinematic cuts eliminating the low $W$ region which might underestimate the values of the higher twist coefficients. Our approach will be of particular relevance to the kinematic regime which will be probed at Jefferson Lab [16–18].

In summary, we analyze the $Q^2$ dependence of the proton structure functions paying particular attention to data at low $Q^2$ and large $x$, i.e., in a region dominated by nucleon resonances. This type of analysis is now possible because more accurate data at large $x$ and relatively low $Q^2$ are becoming available. It is in this way possible both to determine more accurately the coefficients of order $O(1/Q^2)$ contributions and to provide stronger constraints on parameterizations of the parton distributions in this region.

This paper is organized as follows: in Sec. II, we examine in detail the problems that have characterized the large $x$ region, since the early analyses, concerning the role of resonances in QCD, the choice of appropriate scaling variables, and the prescription for target mass corrections. In Sec. III, we describe our procedure for the extraction of power corrections from world DI and resonance data, with particular attention to the problem of defining the parton distributions in the kinematic region of low invariant mass. In Sec. IV, we present and discuss the results. Conclusions are drawn in Sec. V.

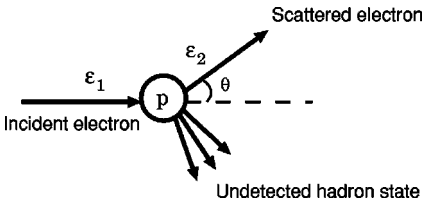


FIG. 1. Schematic diagram of inclusive electron-nucleon scattering.

## II. RESONANCES, SCALING CURVES, AND QCD

In this section, after presenting kinematics and definitions, we summarize what is presently known on the $Q^2$ dependence of the proton structure functions from the elastic, resonant, and deep inelastic regions. We discuss our choice of global parametrization spanning the whole range of measured $x$ and $Q^2$ values including the low final state invariant mass region which is disregarded in current extractions of higher twist corrections. Finally, we examine possible prescriptions for subtracting target mass corrections (TMC) and we present the seemingly best prescription for treating the low final state invariant mass region which again is a problem specifically addressed in this paper and disregarded in most recent analyses.

### A. Kinematics and definitions

Inclusive charged lepton-proton scattering is described in Fig. 1 where the undetected final state can be a proton (elastic scattering), a nucleon resonance state, or a larger invariant mass set of hadrons (deep inelastic scattering). The relevant invariants for this process are

$$Q^2 \equiv (k_1 - k_2)^2 = 4\epsilon_1 \epsilon_2 \sin^2\frac{\theta}{2}, \tag{1a}$$

$$\nu \equiv \frac{(Pq)}{M} = \epsilon_1 - \epsilon_2, \tag{1b}$$

$$x = \frac{Q^2}{2M\nu}, \tag{1c}$$

$$W^2 \equiv (P+q)^2 = M^2 - Q^2 + 2M\nu, \tag{1d}$$

where the momentum components in the laboratory frame are $k_{1(2)} \equiv (\epsilon_{1(2)}, \mathbf{k_{1(2)}})$ for the incident and outgoing electrons; $P \equiv (M,0)$ for the proton target; and $\theta = \hat{\mathbf{k}}_\mathbf{1} \cdot \hat{\mathbf{k}}_\mathbf{2}$ is the scattering angle shown in Fig. 1. The measured electron-nucleon differential cross section can be expressed as

$$\frac{d^2\sigma}{d\Omega d\epsilon_2} = \sigma_M \left( W_2(\nu, Q^2) + 2\tan^2\frac{\theta}{2} W_1(\nu, Q^2) \right), \tag{2}$$

[2]Scaling is defined in [14] modulo the leading twist PCQD corrections.

where $\sigma_M=(4\alpha^2\epsilon_2^2\cos^2\theta/2)(\epsilon_1^2Q^4)$ is the Mott cross section for pointlike scattering. In this paper, we concentrate on the structure function $F_2=\nu W_2(\nu,Q^2)$. This quantity may be written as

$$\nu W_2(\nu,Q^2)=\frac{\nu}{\sigma_M}\left(\frac{d^2\sigma}{d\Omega d\epsilon_2}\right)\frac{1}{1+\beta}; \tag{3}$$

where

$$\beta=2\tan^2(\theta/2)\frac{1+Q^2/4M^2x^2}{1+R}. \tag{4}$$

In this paper, $R=\sigma_L/\sigma_T$, the ratio of the longitudinal to transverse cross sections, has been parametrized as in [10]. $R$ has not been measured with precision better than $\pm 100\%$ at high $x$ and moderate $Q^2$, which introduces an uncertainty in our analysis. This quantity will be measured at Jefferson Lab [19].

The elastic $F_2$ may be expressed as

$$\nu W_2^{el}=\frac{G_E^{p2}(Q^2)+Q^2/4M^2G_M^{p2}(Q^2)}{1+Q^2/4M^2}\delta\left(\nu-\frac{Q^2}{2M}\right), \tag{5}$$

where the electric and magnetic form factors of the proton, $G_E^p$ and $G_M^p=\mu G_E^p$, have been shown to obey basically a dipole behavior

$$F_{dip}=\left(1+\frac{Q^2}{M_o^2}\right)^{-2}, \tag{6}$$

with $M_o^2\approx 0.71$ GeV$^2$. This behavior approaches an $O(1/Q^8)$ dependence at $Q^2>20$ GeV$^2$ [20,21].

### B. Parametrization of $F_2$ in the resonance region

In this section we describe our choice of ''global parametrization,'' spanning through the kinematical regions where relevant data on $F_2$ are available (Fig. 2). The elastic region is denoted (**E**) in Fig. 2 and is represented by a line at $x=1$.

The contribution of resonances to the inelastic structure function is conventionally associated with the region $W<2$ GeV. This is denoted region (**A**) in Fig. 2. Parametrizations that include resonances [22,10,2,23,24] are generally of the form[3]

$$\nu W_2^{inel}=F_S(\zeta)F_{Res}(W,Q^2), \tag{7}$$

where $F_S$ depends only on a dimensionless invariant, $\zeta$, representing different choices of scaling variables ($\zeta=1/\omega'$ [13], $\zeta=1/\omega_p$ [22], $\zeta\approx\xi$ [14]). In all cases, $\zeta\to x$ at high $Q^2$,

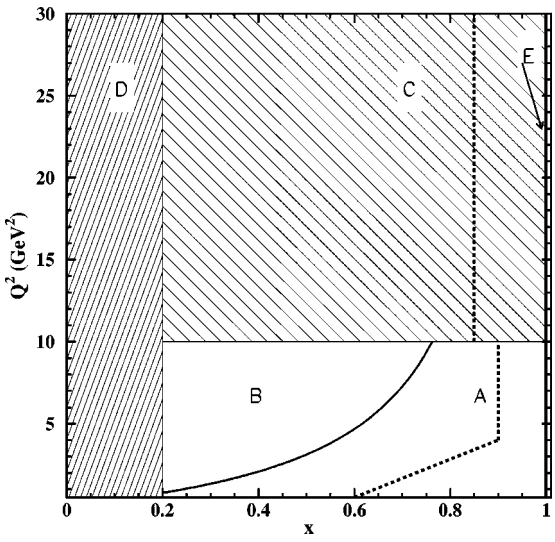


FIG. 2. Kinematical regions covered by the fixed target experiments discussed in the text. Notice that data are available up to $Q^2\approx 200$ GeV$^2$ in region C and that the maximum value of $Q^2=30$ GeV$^2$ is chosen in the figure for the purpose of better evidentiating the resonance region and of keeping at the same time an ''ensemble'' picture of the data.

will be discussed, and $F_{Res}$ is parametrized as a sum of Breit-Wigner terms to which a smooth nonresonant background is added:

$$F_{Res}(W,Q^2)=F_{BW}(W,Q^2)+F_{\rm BKG}(W,Q^2). \tag{8}$$

$F_{\rm BKG}(W,Q^2)$ depends only on $W$ in most parametrizations, but not in the newest ones [2,24]. The $Q^2$ behavior of resonances, except for the anomalous case of the $\Delta$ [23], follows a $1/Q^4$ decrease of the resonance peak above $Q^2\approx 2$ GeV$^2$, in agreement with early dimensional scaling predictions (see, e.g., Ref. [25]). Early literature on the subject is focused on the integrals of $\nu W_2^{inel}$ over well-defined intervals of $\zeta$. These integrals have been found to decrease with $Q^2$ at the same rate as their correspondent quantities in the DI region, thus satisfying a FESR consistent with the duality ideas of Bloom and Gilman (BG) [12]. This behavior is reproduced by parameterizations of the type of Eq. (7) where the $Q^2$ dependences of both the resonance peaks and of the duality integrals are consistent with the $Q^2$ dependence of $F_S(\zeta)$, once $\zeta$ is calculated at a fixed $W$ (e.g., $W\equiv W_{peak}$). In this paper, part of this observation is utilized in that, as explained in detail below, the power corrections to the DI structure function are extracted as small scale deviations from the FESR. It will be shown quantitatively how the integrals defining the FESR are numerically close to the integrals defining the moments of the structure function in QCD.

At $W\approx 2$ GeV, the resonance region parametrizations typically connect smoothly with the DI ones. DI parametrizations [9] reproduce accurately the $Q^2$ behavior of $F_2$ predicted by next-to-leading order (NLO) QCD evolution. We have classified the corresponding kinematic domains in Fig. 2 as region (**B**) for $W\geqslant 2$ GeV and $Q^2\leqslant 10$ GeV$^2$ and region (**C**) for $W\geqslant 2$ GeV and $Q^2\geqslant 10$ GeV$^2$, according to

[3]Only the most recent parametrizations are quoted, and their main features highlighted. For details, we refer the reader to the referenced papers.

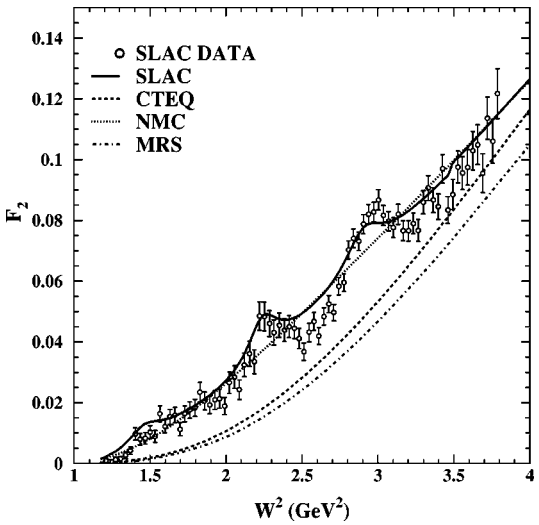


FIG. 3. Proton structure function in region (**A**). $Q^2$ for the SLAC data is between 4 and 5 GeV$^2$ and $x$ is between 0.55 and 0.95.

the availability of parametrizations from different sets of data, as explained below. Here, Eq. (7) is dominated by the smooth function $F_S$ and $\zeta$ is identified with $x$. Figure 2 also shows the kinematic domain (**D**) which corresponds to the very low $x$ ($x<0.2$) region. The region on the larger $x$ side of the dashed line in Fig. 2 represents a kinematic region for which no data are currently available. There also exists a region of very small $x$ where there are no data available ($x<0.000032$ [26]). As will become clear from the following, it would be extremely valuable for the understanding both of power corrections and more generally of the physics at the border between PQCD and nonperturbative QCD, to perform actual measurements in these regions.

An overview of world parametrizations in the kinematic regions A–D are shown in Figs. 3 to 6 compared to data. In the large $x$ and moderate $Q^2$ region (**A**), the bulk of the data

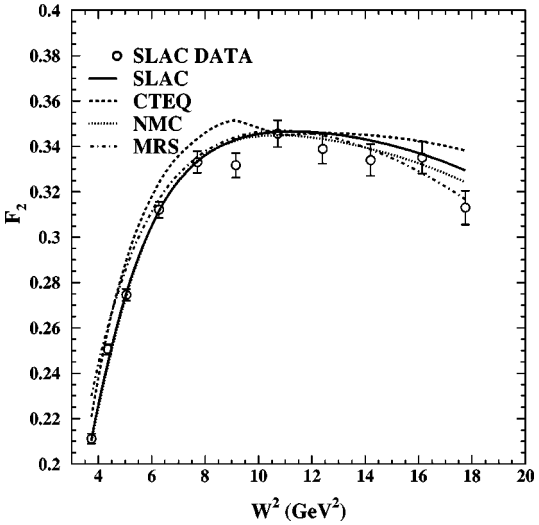


FIG. 4. Proton structure function in region (**B**). $Q^2$ for the SLAC data is between 1.1 and 2.3 GeV$^2$ and $x$ is between 0.06 and 0.45.

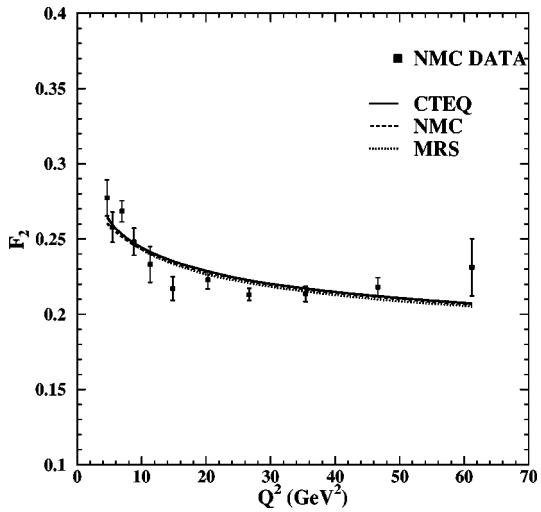


FIG. 5. Proton structure function in region (**C**). The NMC data are for $x=0.35$.

are from older SLAC experiments (for example, [22,27]) which have no better than 5% precision. However, there do exist a few newer and higher precision data ( [2,3,24,28,29]) sets in this region. In regions (**A**) and (**B**), several parametrizations are available. In Figs. 3 and 4, four models are compared with data obtained from SLAC: two parametrizations obtained using mainly SLAC data [2,10] and three parametrizations obtained using world data [CTEQ4 [30], Martin-Roberts-Stirling (MRS) [31], and New Muon Collobration (NMC) [32]].

The choice of parametrization for the high $x$ and moderate $Q^2$ region is of particular importance to this analysis, as it is here that the higher twist effects are expected to be largest. For this region, we utilized a new global fit (shown in Fig. 3) to all inclusive data from SLAC ( [2,24]). This is the only fit available which represents the entire three decades of data available from SLAC and it has predicted within a few percent the new Jefferson Lab cross sections which are typically

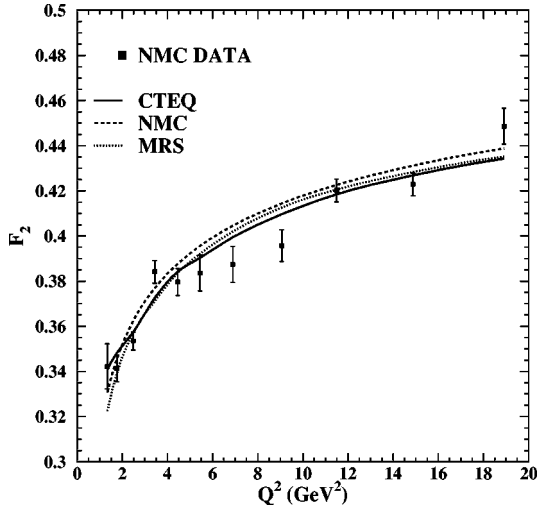


FIG. 6. Proton structure function in region (**D**). The NMC data are for $x=0.05$.

an order of magnitude more precise than any inclusive measurements available in this region [16,28]. To develop this reliable global model of inclusive resonance electroproduction, some of the much older data were reanalyzed and corrected where applicable to reflect, for instance, more thorough radiative corrections and normalizations to accurate deep inelastic data. The fit was constrained to smoothly match the Whitlow ( [10]) fit to deep inelastic data throughout the similar moderate $Q^2$ range. The behavior of the structure function as a function of $Q^2$ for different values of $x$ in regions (**C**) and (**D**) is shown in Figs. 5 and 6. The curves were obtained using different existing models [30–32]. Here, the SLAC models are no longer valid. It should be finally noticed that the bulk of data on $F_2^p$ has been obtained for the kinematics of regions (**C**) and (**D**) where several experimental results overlap.

### C. Target mass corrections

At large enough values of $W$ and $Q^2$ (i.e., in regions B–D of Fig. 2), QCD provides a clear and rigorous description of the physics that generates the $Q^2$ behavior of the nucleon structure function. At leading twist (LT), it is possible to relate the moments of order $n$ of the structure function,

$$M_n(Q^2)=\int_0^1 dx F_2(x,Q^2)x^{n-2}, \tag{9}$$

to products of the matrix elements of spin $n$ operators calculated at a scale $\mu^2$ times the ($Q^2$-dependent) Wilson coefficient functions. The $Q^2$ dependence of such functions is calculated by solving the well-known renormalization group equations. Moreover, there is also a clear connection with the language of the parton model and Bjorken $x$ clearly emerges as the correct scaling variable (see [5,6]).

When $W\to M$, the simplicity of the aforementioned picture is no longer attainable. Because of the occurrence of finite target mass terms, one can no longer make a one to one correspondence between the ''$n$'' moments of the structure function and the spin of the operators in the operators producet expansion (OPE). Both kinematical power corrections, or TMC and dynamical power corrections have to be simultaneously taken into account and the expression for the moments becomes [33]

$$M_n(Q^2)=M_n^{LT}(Q^2)+f_n^{kin}(Q^2)\frac{M^2}{Q^2} + H_n^{(4)}(Q^2)\frac{1}{Q^2}+O(1/Q^4)+\cdots. \tag{10}$$

The kinematical power corrections cannot be handled in a completely model independent way because of the off-shellness of the quarks participating in the scattering process. This limits the extent to which kinematical and dynamical power corrections can be extracted separately from experimental data, in particular, in the low $Q^2$ and $W$ regime addressed in this paper. We will fully address this theoretical point in a forthcoming paper [34]. Here, as our goal is to assess the feasibility of a perturbative QCD based extraction of the higher twist terms in the kinematical regime accessible at Jefferson Lab, we take into account TMC (i.e., the kinematical power corrections) by evaluating the Nachtmann moments of $F_2$ [35]. In this way, the magnitude of the dynamical power corrections obtained in our analysis can be compared unambigously to the results of other recent extractions using the same prescription [15]. The theoretical uncertainties in the determination of TMC are incorporated in a ''theoretical'' systematic error. Nachtmann moments take into account TMC at all orders in $M^2/Q^2$ [35]. They are derived assuming on-shell quarks. Their expression for $F_2$ is

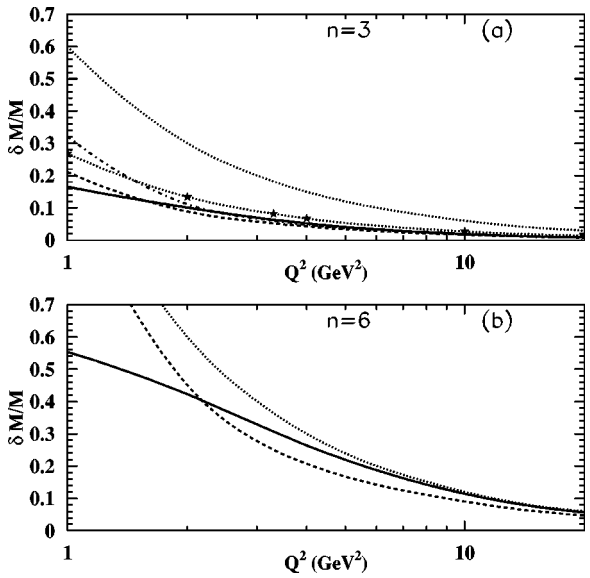


FIG. 7. Percentage contribution of TMC to the structure function moments, calculated according to the models discussed in the text. For a clearer presentation, all models discussed in the text are compared in (a) whereas in (b) $n=6$ we show only the Nachtmann contribution along with the $M^4/Q^4$ term discussed in the text. For comparison, we plot also an estimate of the HT contributions which is of the order obtained in our analysis (see Sec. III).

$$M_n^N(Q^2)=\int_0^1 dx\frac{\xi^{n+1}}{x^3}\times\left(\frac{3+3(n+1)r+n(n+2)r^2}{(n+2)(n+3)}\right)F_2(x,Q^2), \tag{11}$$

where

$$r=\left(1+\frac{4M^2x^2}{Q^2}\right)^{1/2} \quad \text{and} \quad \xi=\frac{2x}{1+r}. \tag{12}$$

In order to show the behavior of TMC in the region of interest and to test the relevance of possible off-shell contributions, in Fig. 7 we present the percentage contribution of TMC calculated according to different models. This is defined by the ratio

$$\frac{\delta M}{M} = \frac{M_n - M_n^{TMC}}{M_n}, \tag{13}$$

where $M_n^{TMC}$ includes target mass corrections and $M_n$ is the moment defined in Eq. (9). The TMC calculations in Fig. 7a are from Ref. [35] (full line), $M_n^{TMC}$ being also defined in Eq. (11), and from Ref. [36] (dashed and dot-dashed lines). The latter retain the $M^2/Q^2$ term (dashed line) and the $M^4/Q^4$ (dot-dashed line) term in the power series defined in Eq. (10) [37], thus, avoiding the well-known problem of the unphysical threshold at $\xi \equiv \xi_p = 2/(1+\sqrt{1+4M^2/Q^2}) < 1, x = 1$ (see discussion in [38,36]). It is clear that at low $Q^2$, the power expansion form of TMC cannot be applied because of the large size of the expansion parameter. We also present an estimate of the off-shell corrections obtained following the model of Ref. [33] for the nonsinglet case (stars): this contribution is sensibly larger than the Nachtmann moment one for $Q^2 \leqslant 3$ GeV$^2$. Finally, all of the above ''non-QCD'' $Q^2$-dependent corrections are compared with an estimate of the dynamical power correction (dotted line) extracted from the data (see next section). In Fig. 7(b) we show the percentage contribution from the Nachtmann moment along with the approximated form of Ref. [36] and the estimated dynamical power correction at a larger value of $n$. Our conclusion is that TMC can be separated from the dynamical power corrections provided the uncertainty which is introduced in the theoretical evaluation of TMC is properly accounted for by a ''theoretical'' systematic error. This procedure can be applied when the systematic error is small compared to the magnitude of the power corrections i.e., at $Q^2 \gtrsim 3$ GeV$^2$ and $n < 8$.

Having accounted for TMC, one can write a twist expansion form for the moments defined above which schematically reads

$$M_n(Q^2) = M_n^{PQCD}(Q^2) + \frac{\tau^2(n)}{Q^2} A_n^{(2)}(Q^2) + \frac{\gamma^4(n)}{Q^4} A_n^{(4)}(Q^2) + \cdots, \tag{14}$$

where we define $M_n^{PQCD}(Q^2)$ as the LT part. The $\tau^2(n)$ and $\gamma^4(n)$ coefficients are to be determined by experiment, and the $A_n^{(2,4)}(Q^2)$ are (to this date unknown) perturbative coefficients of the power correction terms (see however [11]).

The determination of the size of $\tau^2(n)$ has been the subject of many investigations and it is a primary goal of the present paper. The main obstacle to an accurate extraction of this quantity from data is that $O(1/Q^2)$ and higher terms are largest at large $x$ and low $Q^2$ where the cross section is determined largely by resonances (see Fig. 9 in [39]), which are in principle entirely nonperturbative effects. Two important QCD-based quantitative analyses including the resonance region are in [14] and in [39]; other recent extractions of higher twist corrections do not include the resonance region. For example, the analysis of [15] considers cuts at $x \gtrsim 0.75$, corresponding to $W \gtrsim 2$ GeV. By applying these cuts, one might underestimate the size of the higher twist coefficients as defined in Eq. (14). Moreover, there is no intrinsic reason why such cuts should be applied. Our main results are in fact that i the resonance region can be included in the PQCD analysis by using moments and the phenomenolgical observation of BG duality, and i the resonance region, one obtains a much larger value of the HT coefficients than in previous analyses.

In the following sections, we present results from a new analysis based on the moments of the structure function. By using moments, it is possible to integrate data directly with no assumptions and we do not depend on any assumption underlying the choice of curve which crosses the low $W$ region including the resonance peaks. At the same time, as can be seen from the definition in Eq. (9), the importance of the large $x$ region is weighed by considering moments of increasingly large $n$. This analysis provides a clearcut approach for disentangling the different power corrections: the TMC, or kinematic corrections, and the dynamic corrections generated by multiparton interactions. We also obtain a constraint on the LT parton distributions used as input for QCD evolution at large $x$ and large $Q^2$. This result provides an alternative to approaches utilizing it ad hoc low $Q^2$ input distributions, constructed in such a way that after evolution, they agree with higher $Q^2$ data. Although large variations in the large $x$ tail of the valence quark distributions at low $Q^2$ do not influence the distributions at the larger $Q^2$ values where the bulk of data lie ($Q^2 \lesssim 300$ GeV$^2$), they might lead to substantial variations at *very large* $Q^2$ ($Q^2 \approx 10^4$ GeV$^2$), a regime now accessible at HERA.

## III. EXTRACTION OF THE HIGHER TWIST COEFFICIENTS

In this section, we discuss in detail our analysis of the large $x$ behavior of the proton structure function and of the coefficients of the power corrections. Since we are mainly interested in the large $x$ region, we concentrate on the flavor nonsinglet (NS) part of the structure function that is known to dominate largely the moments of $F_2^p$ for $n \geqslant 4$ [40]. The $Q^2$ dependence of the NS moments at NLO in the modfied minimal subtraction (MS) scheme, is predicted to be

$$M_n^{NS}(Q^2) = \overline{M}_n^{NS} [\ln(Q^2/\Lambda^2)]^{-d_n^{NS}} \left(1 + \frac{R_n^{NS}(Q^2)}{\beta_o \ln(Q^2/\Lambda^2)}\right), \tag{15}$$

where $R_n^{NS}(Q^2) = R_n^{NS} - \beta_1/\beta_o d_n^{NS} \ln\ln(Q^2/\Lambda^2)$, $R_n^{NS}, \beta_o, \beta_1$, and $d_n^{NS} = \gamma_n/2\beta_o$ are calculated constants (see [6] and references therein); The NS anomalous dimensions are the $\gamma_n$. For our purpose, it is convenient to write [41]:

$$[M_n^{NS}(Q^2)]^{-1/d_n^{NS}} \propto (\ln Q^2 - \ln \Lambda^2)(\text{higher order terms}). \tag{16}$$

A plot of Eq. (16) vs $\ln Q^2$ shows that: (i) LO PQCD behavior is given by a straight line with possible small corrections from higher order terms; and (ii) large deviations from a straight line at low $Q^2$ can be mainly ascribed to power corrections.

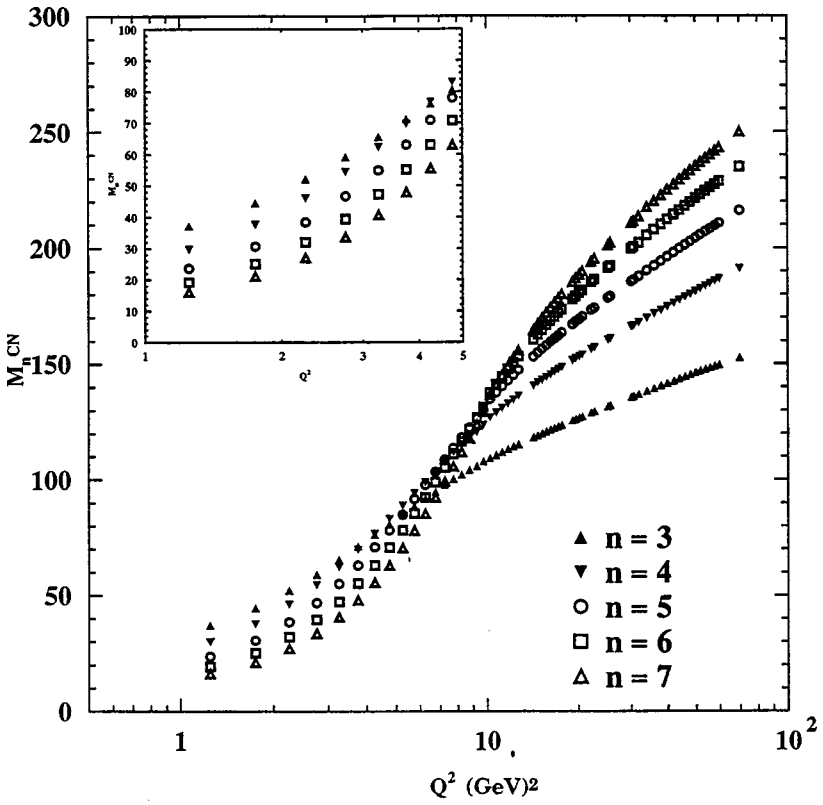


FIG. 8. Cornwall-Norton moments. The inset represents the low $Q^2$ region.

In order to calculate the moments, one needs to integrate the proton structure function $F_2$ in the entire region $0<x<1$. Additionally, to obtain the $Q^2$ dependence of these moments, the integrals should be calculated at different $Q^2$ for the same 0 to 1 range in $x$. This implies that reliable data or parametrization(s) of available data are available which cover a wide range of both momentum transfer as well as $0<x<1$. No single experiment covers these ranges in $x$ and $Q^2$ simultaneously. Therefore, reliable parametrizations are needed to obtain the integrals in Eqs. (9) and (11). There are at present several parametrizations of the structure function (summarized in [9]), where mostly deep inelastic data were used. The high $x$, low $Q^2$ region, the resonance region, is poorly represented.

To estimate the contribution of various $x$ regions to the moments, let us define two additional integrals:

$$I_n(x_{lim},1)=\int_{x_{lim}}^{1} dx \;\; F_2(x)x^{n-2} \tag{17}$$

and

$$I_n(0,x_{lim})=\int_{0}^{x_{lim}} dx \;\; F_2(x)x^{n-2}. \tag{18}$$

In Fig. 8 we show the ratio $I_n(0,x_{lim})/M_n$ for the Cornwall-Norton moments at $Q^2=10$ GeV$^2$ and several values of $n$. From this plot, one can see that the lower moments are very sensitive to the low $x$ region. For example, for $n=2$, the $x<0.2$ region gives about 50% of the moment for the $Q^2$ considered. As $n$ increases, the contribution of the small $x$ domain becomes less important (less than 1% for $n=6$ and $x_{lim}=0.2$). The high $x$ region is more important for higher moments. The region above $x=0.7$ contributes about 15% for $n=4$ and less than 5% for $n=2$. The elastic contribution ($x=1$) was not included in the integrals; it is is more important for lower $Q^2$(6% of $M_2$ for $Q^2=2.6$ and only 0.3% for $Q^2=10$).

To select the best structure function representation for the whole kinematic domain required to evaluate the QCD moments at different $Q^2$'s, we divided the $(x,Q^2)$ space into several regions (Fig. 2): (**A**) the resonance region of $Q^2 \in (0.5,10.0)$ GeV,$x\in(0.2,1.0)$, and $W^2<4.0$; (**B**) the DIS low $Q^2$ region of $Q^2\in(0.5,10.0)$ GeV, $x\in(0.2,1.0)$, and $W^2>4.0$; (**C**) the DIS high $Q^2$, $Q^2>10.0$ GeV; (**D**) the low $x$ region of $x<0.2$; and (**E**) the elastic scattering region, $x=1.0$. The structure function for region (**E**), elastic scattering, was obtained using the Gari-Krümpelmann parameterization for the proton magnetic form factor $G_{Mp}$ [42] and the dipole parametrization for the proton electric form factor $G_{Ep}$. Regions (**A**) to (**D**) are described in Sec. II. In this analysis, we use the SLAC model ( [2,10], solid lines in Figs. 3 and 4) for regions (**A**) and (**B**) and the NMC parametrization [34], the dashed lines in Figs. 5 and 6 for regions (**C**) and (**D**).

Using the parametrizations outlined above and Eqs. (9) and (11), we obtained the moments in Figs. 9 and 10. The insert in both figures represents the low $Q^2$($Q^2<5$ GeV$^2$) behavior of the moments. For $Q^2\gtrsim 20$ GeV$^2$, the moments depend linearly on $\ln Q^2$, as expected from Eq. (15). In the low $Q^2$ region, we observe a deviation from this linear de-

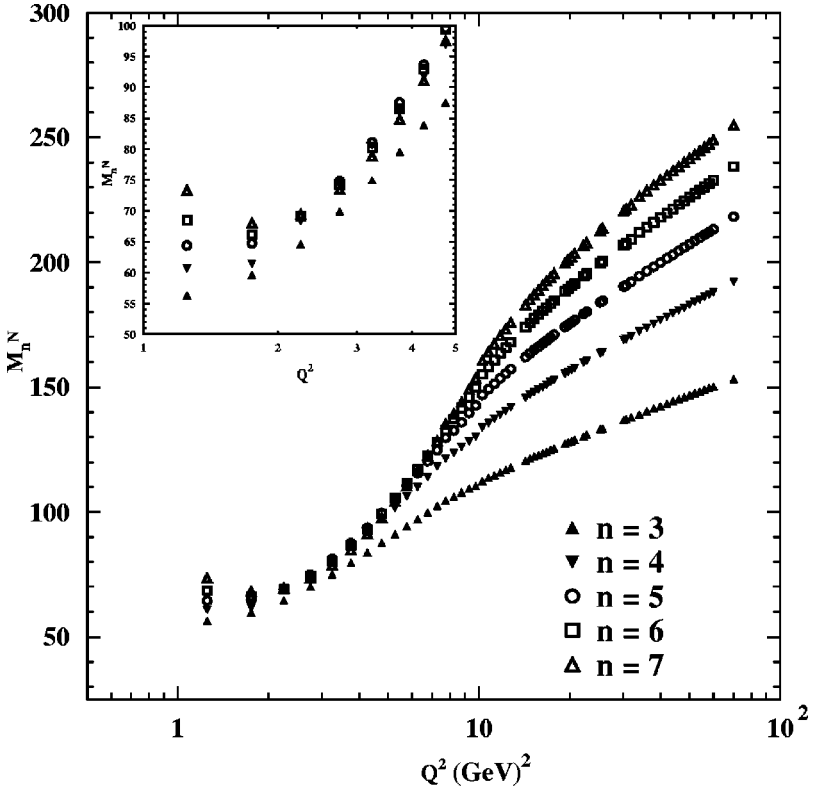


FIG. 9. Nachtmann moments. The inset represents the low $Q^2$ region.

pendence, due to higher twist effects. This deviation is less pronounced in Fig. 10 where the target mass effects have been accounted for as described in Sec. II.

Based on Eqs. (14), (15), and (16), we used the following expression to fit the moments in Figs. 9 and 10:

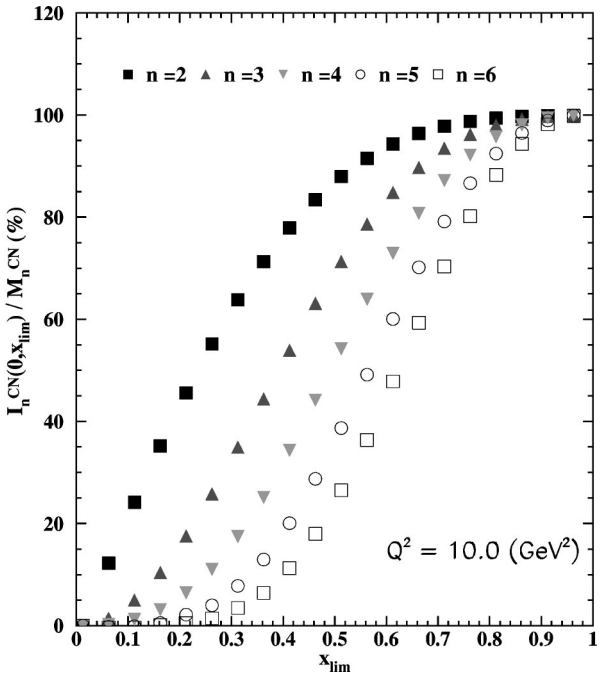


FIG. 10. High $x$ region contribution to moments.

$$M_n(Q^2)^{-1/d_n} = M_n^{PQCD}(Q^2)^{-1/d_n}\left(1+\frac{P2}{Q^2}\frac{P3}{Q^4}\right)^{-1/d_n}, \tag{19}$$

where

$$M_n^{PQCD}(Q^2)^{-1/d_n} = P1\ln\left(\frac{Q^2}{\Lambda^2}\right)(1+\text{h.o.})^{-1/d_n}. \tag{20}$$

Equation (19) corresponds to the approximation $A_n^{(2)} \approx A_n^{(4)} \approx M_n^{PQCD}$ in the twist expansion (14), which we define as the *factorized form*. We adopted this approximation in order to be consistent with previous evaluations ([13] in $n$-space and [15] in $x$-space). $P1$,$P2$, and $P3$ are ($n$-dependent) parameters which can be obtained by fitting $M_n(Q^2)$ as a function of $\ln Q^2$. $\Lambda$ is also a parameter of the fit centered around 250 MeV, in agreement with previous results [15,31]. The first term, $P1$, is determined by the high $Q^2$ region where PQCD effects are dominant and the higher twist effects are negligible. The other terms, $P2$ and $P3$, can be related to the higher twist effects. We stress again that the main point of this paper is to underline the importance of the resonance region in the determination of the HT coefficients and to define an approach to incorporate it in the analysis. A more detailed analysis showing, e.g., results using different models besides the one in Eq. (19) will be presented elsewhere [43].

The results of the present fit are given in Tables I and II. In order to fix the high $Q^2$ behavior of the moments, we first fit the leading term in Eq. (19) for $n=3$, 4, 5, 6, and 7 for

TABLE I. Leading order term ($P1$) and higher order terms ($P2$ and $P3$) in Eq. (19) for the Cornwal-Norton moments. The uncertainties quoted are results from the fit. Notice that the $n$ dependence of the parameters has not been subtracted.

| n | $P1$ | $\delta P1$ | $P2$ | $\delta P2$ | $P3$ | $\delta P3$ |
|---|---|---|---|---|---|---|
| 3 | 21.66 | 0.18 | −0.14 | 0.04 | 3.06 | 0.50 |
| 4 | 27.46 | 0.25 | −0.15 | 0.06 | 9.58 | 0.67 |
| 5 | 31.34 | 0.30 | −0.31 | 0.11 | 19.75 | 1.04 |
| 6 | 34.31 | 0.35 | −0.65 | 0.10 | 33.50 | 1.25 |
| 7 | 36.73 | 0.40 | 1.54 | 0.11 | 35.50 | 1.42 |

$Q^2$ between 20 and 75 GeV$^2$. To verify the stability of the fit, we varied the low $Q^2$ limit from 20 to 40 GeV$^2$. The dependence of $P1$ on this lower $Q^2$ limit is shown in Fig. 11.

The two terms $P2$ and $P3$ were obtained by fitting the moments including the low $Q^2$ region (2 to 10 GeV$^2$). In Table I we present our values for all three parameters for the Cornwall-Norton moments, whereas in Table II we present Nachtmann moment parameter values with TMC subtracted according to the procedure described in Sec. II. These values correspond to $Q^2_{\rm min}=4$ GeV$^2$, a value that we will discuss in Sec. IV. Below $Q^2=2$ GeV$^2$, Eq. (19) does not reproduce the data very well; the moments turn upward and the contributions from the $1/Q^2$ and $1/Q^4$ terms do not reproduce this feature. In this very low $Q^2$ region, the twist expansion as given in Eq. (14) is likely to break down. The introduction of a fourth term in Eq. (19), $P4/Q^6$, improves the fit, but the uncertainty on P4 is large.

## IV. DISCUSSION OF NUMERICAL RESULTS

In this section we discuss the coefficients obtained by fitting the moments of $F_2^p$ with Eq. (19). Our results are shown in Tables I–IV. Tables I and II include data with a minimum $Q^2$ cut of 4 GeV$^2$, the value at which the dependence of the parameters on such a cut becomes negligible. Results in Tables III and IV correspond to a minimum $Q^2$ cut of 2 GeV$^2$, which, as explained above, is a minimum value for which our QCD analysis is applicable. The errors, $\delta P1$, $\delta P2$, and $\delta P3$, are obtained from the fit, assuming a 3% uncertainty for the calculated moments. This uncertainty is based on the accuracy of the data from which the different parameterizations were obtained, and is comparable to what was used in previous papers (for example, [11]).

As mentioned above, $P1$ is determined by the high-$Q^2$ data and is related to the logarithmic scaling violation. Thus,

TABLE II. Same as in Table I, but for the Nachtmann moments.

| n | $P1$ | $\delta P1$ | $P2$ | $\delta P2$ | $P3$ | $\delta P3$ |
|---|---|---|---|---|---|---|
| 3 | 21.87 | 0.19 | −0.55 | 0.06 | 4.38 | 0.66 |
| 4 | 27.05 | 0.24 | −0.01 | 0.03 | 4.50 | 0.80 |
| 5 | 30.42 | 0.27 | 0.28 | 0.08 | 6.72 | 2.10 |
| 6 | 32.94 | 0.30 | 0.40 | 0.10 | 11.24 | 1.70 |
| 7 | 36.80 | 0.40 | 0.41 | 0.11 | 17.77 | 1.80 |

TABLE III. Higher order terms ($P2$ and $P3$) in Eq. (19) for the Cornwall-Norton moments with a lower cut at $Q^2=2.0$ GeV$^2$.

| n | $P2$ | $\delta P2$ | $P3$ | $\delta P3$ |
|---|---|---|---|---|
| 3 | 0.02 | 0.03 | 1.84 | 0.12 |
| 4 | 0.33 | 0.04 | 4.69 | 0.19 |
| 5 | 0.46 | 0.05 | 10.57 | 0.29 |
| 6 | 0.36 | 0.07 | 20.90 | 0.43 |
| 7 | 1.97 | 0.08 | 30.87 | 0.60 |

$P1$ determined from Cornwall-Norton moments should be comparable to $P1$ determined from Nachtmann moments because TMC effects are small in this $Q^2$ range. This is verified in Tables I and II.

The TMC effects become important for $2\leqslant Q^2 \leqslant 10$ GeV$^2$, where we extract the higher twist coefficients $P2$ and $P3$. In this case, we expect $P2$ and $P3$ extracted from the Cornwall-Norton moments to be larger than those obtained from the Nachtmann moments since, in the latter case, the TMC effects are taken into account. Having the same $1/Q^2$ behavior, TMC effects and higher twist effects cannot be separated using Eq. (19). This expected behavior is observed for $P2$ and $P3$ in our analysis. In the present analysis, $P2$ is occasionally negative. As noted in Ref. [41], there is no *a priori* theoretical constraint that will force $P2$ to be positive.

In order to compare our results to previous efforts, we choose a model for the $n$ dependence. Namely, we assume in the factorized form of Eq. (14) that:

$$\tau^2(n)=n\tau^2, \quad \text{and} \quad \gamma^4(n)=n^2\gamma^4. \tag{21}$$

We do not however require $(n^2\gamma^4)$ to equal $(n\tau^2)^2$, differing from [14]. Equation (21) corresponds to the dominance of two-fermion diagrams over four-fermion diagrams in the evaluation of higher twists contributions [14,44]. It is used in many of the previous extractions using moments [14,41] and it is also consistent with some of the extractions using the structure function [15] directly because it corresponds to an anti-Mellin transform behavior of the type $\propto 1/(1-x)$. It is important to notice that all of the quoted determinations do not include the $O(1/Q^4)$ terms.

Within our choice for the $n$-dependence, we obtain: $\tau^2 = 0.06\pm 0.02$ and $\gamma^4=0.30\pm 0.07$, where the average over $n$, for $n=4-7$, is taken and $Q^2_{\rm min}=4$ GeV$^2$. With a lower cut in

TABLE IV. Same as in Table III, but for the Nachtmann moments.

| n | $P2$ | $\delta P2$ | $P3$ | $\delta P3$ |
|---|---|---|---|---|
| 3 | −0.24 | 0.03 | 1.54 | 0.11 |
| 4 | 0.33 | 0.04 | 1.61 | 0.15 |
| 5 | 0.80 | 0.05 | 2.38 | 0.21 |
| 6 | 1.21 | 0.06 | 3.79 | 0.27 |
| 7 | 1.60 | 0.07 | 5.86 | 0.36 |

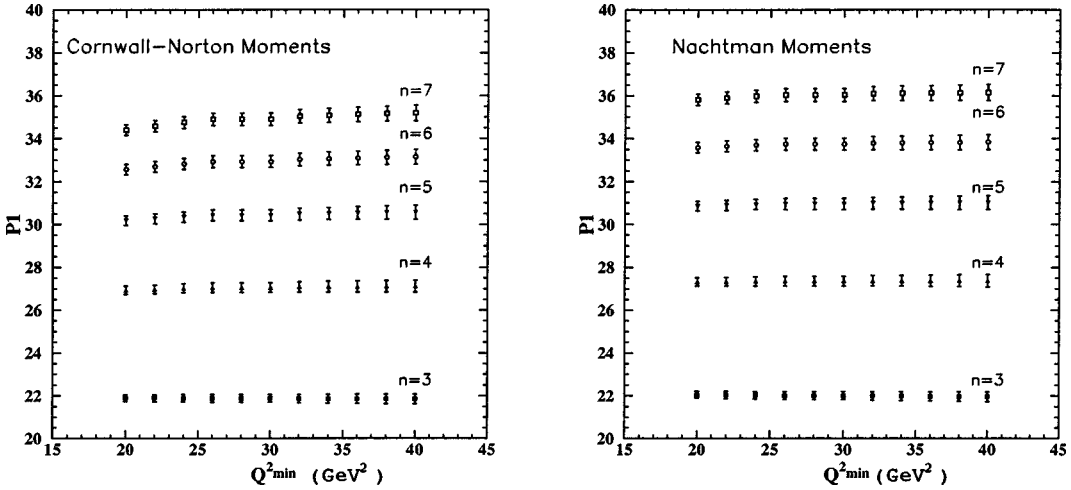


FIG. 11. Leading order term, $P1$ in Eq. (19) as a function of the minimum $Q^2$ used in the fit.

$Q^2$, $Q^2_{\rm min}=2$ GeV$^2$, we obtain: $\tau^2=0.20\pm0.02$ and $\gamma^4=0.11\pm0.01$. Our choice for the range in $n$ is determined by the lowest value at which we can disregard the singlet contributions without introducing a large systematic uncertainty (i.e., $n\geqslant 4$), and by the highest limit, (i.e., $n\approx 7-8$) for which the higher twist terms satisfy the conditions $n\tau^2/Q^2 \ll 1$ and $n^2\gamma^4/Q^4 \ll 1$ at all values of $Q^2$ considered [14]. We were also careful that the region where experimental data are missing (see Fig. 2) did not contribute sensibly.

Once the PQCD parameters $P1$ and $\Lambda$ are fixed, we observe a correlation between the $O(1/Q^2)$ and $O(1/Q^4)$ parameters: $P2\equiv n\tau^2$ and $P3\equiv n^2\gamma^4$, respectively. We obtain consistent $\chi^2$ values both with a rather small value of $\tau^2$ and a large value of $\gamma^4$ at $Q^2_{\rm min}=4$ GeV$^2$, and with a larger value of $\tau^2$ and a consequently diminished value of $\gamma^4$ at $Q^2_{\rm min}=2$ GeV$^2$.

As stated in Sec. II, there exist a number of investigations of higher twist effects in inclusive scattering data using PQCD based approaches. The primary assumptions in these analyses are summarized below and, where appropriate, relevant numerical values are compared with the results of the present work.

(1) De Rujula, Georgi, Politzer [14]: The twist expansion for the Nachtmann moments corresponds to the factorized form, with an $n$ dependence as in Eq. (21). The PQCD analysis was performed up to LO and only the $O(1/Q^2)$ term was included. The value of $\tau^2$ is $\approx 0.16$ GeV$^2$. No uncertainties are quoted in this paper.

(2) Pennington, Ross [41]: The form for fitting the moments is:

$$M_n(Q^2)=M_n^{QCD}(Q^2)\left(1+\frac{n\tau^2}{Q^2}\right) \tag{22}$$

which is essentially Eq. (19) up to the order $1/Q^2$. The value for $\tau^2$ is $\sim 0.03^{+0.22}_{-0.13}$ GeV$^2$. This result, represents one of the first quantitative analysis (in addition to the early evaluation of [39]) studying the correlation between the PQCD parameters and the higher twist coefficients (see also Ref. [40]).

(3) Virchaux, Milzstajn [15]: In this work the structure functions are fitted rather than the QCD moments. The form used for this fit is

$$F_2^{HT}(x_i,Q^2)=F_2^{LT}(x_i,Q^2)\left(1+\frac{C_i}{Q^2}\right). \tag{23}$$

The data used for the fit did not include resonance region data. The coefficient $C_i$ varies between $-0.1$ for $x=0.07$ to 1.25 for $x=0.75$, i.e., it has a sharp increase with $x$. By calculating the Mellin transform of Eq. (23), we obtain a rather constant behavior of the coefficient $\tau^2$ with $n$, averaged around 0.1 GeV$^2$. We quote no error bar for this value, due to the large systematic uncertainty at $x>0.75$.

(4) Ji, Unrau [11]: The form for the twist expansion is again Eq. (14). In this paper only the twist-4 terms were fitted. The results for $\sqrt{\tau^2}$ ranged from 0.26 GeV to 0.69 GeV when the order of the moment varied from 2 to 10. No error bars are given.

(5) Cothran, Day, Liuti [45]: This is the first attempt to extract higher twist terms from inclusive electron scattering data for large nuclei. DI electron-nucleus data can be extended more easily to larger values of $x$. The moments were fitted using Eq. (19) up to order $1/Q^2$ and the mass parameter $\tau^2$ is $0.2\pm0.07$ GeV$^2$ in the range $n=4-7$.

Although other analyses exist, we selected the ones that allowed a significant comparison with our approach. For a more extended list of previous works, see [46].

## V. CONCLUSIONS

Our analysis of the QCD moments of the structure function properly includes the resonance region, takes care of spurious kinematic effects such as target mass corrections, and keeps a low minimum value of $Q^2\approx 2$ GeV$^2$. We conclude that: (i) power correction terms up to order $1/Q^4$ are important, but higher order terms may be disregarded. This indicates that a quantitative, QCD based analysis is possible. (ii) Further, the values of the higher twist coefficients ex-

tracted are much larger than those obtained when cuts on low invariant mass data are applied. A larger value of the $1/Q^2$ coefficient is observed in analyses of the type of Refs. [45] and [11], where $O(1/Q^4)$ terms were not considered. Our results show that data can be interpreted in terms of an important positive contribution from the $1/Q^4$ term and a rather small contribution from the $1/Q^2$ coefficient. This implies a correlation between power corrections of different order that cannot be disentangled using the presently available data. We hope that this study will encourage further experimental investigations on the large $x$ behavior of the proton structure function.

## ACKNOWLEDGMENTS

This work was funded by the N.S.F. (Grant No. PHY-9633750 and PHY-9600208) and by D.O.E. (Grant No. DEF-G05-91ER40620). S.L. thanks the Institute of Nuclear and Particle Physics at the University of Virginia for support and the Nuclear Physics Theory Division at Argonne National Laboratory where this manuscript was completed.

[1] P. Bosted *et al.*, Phys. Rev. D **49**, 3091 (1994).
[2] C. Keppel, in Proceedings of the Workshop on CEBAF at Higher Energies, 1994, edited by N. Isgur and P. Stoler, 1994, p. 237.
[3] I. Niculescu, Ph.D. thesis, Hampton University, 1999.
[4] H1 Collaboration, C. Adloff *et al.*, Z. Phys. C **74**, 191 (1997); ZEUS Collaboration, *ibid.* **74**, 207 (1997).
[5] G. Altarelli, Phys. Rep. **81**, 1 (1982).
[6] A.J. Buras, Rev. Mod. Phys. **52**, 199 (1980).
[7] S. Kuhlmann, H.L. Lai, and W.K. Tung, Phys. Lett. B **409**, 271 (1997).
[8] P. Bosted and S. Rock, hep-ph/9706436.
[9] H. Plothow-Besch, PDFLIB Version 7.09-W5051, CERN-PPE 1997.07.02, CERN Computer Program Library Office.
[10] L.W. Whitlow, E.M. Riordan, S. Dasu, S. Rock, and A. Bodek, Phys. Lett. B **282**, 475 (1992).
[11] X. Ji and P. Unrau, Phys. Rev. D **52**, 72 (1995).
[12] P.D.B. Collins, *An Introduction to Regge Theory and High Energy Physics* (Cambridge University Press, Cambridge, England, 1977).
[13] E.D. Bloom and F.J. Gilman, Phys. Rev. D **4**, 2901 (1971); Phys. Rev. Lett. **25**, 1140 (1970).
[14] A. De Rujula, H. Georgi, and H.D. Politzer, Ann. Phys. (N.Y.) **103**, 315 (1977); Phys. Lett. **64B**, 428 (1977).
[15] M. Virchaux and A. Milzstajn, Phys. Lett. **74B**, 221 (1992).
[16] C. Keppel *et al.*, approved Jefferson Lab experiment, E97010.
[17] Z. Meziani *et al.*, approved Jefferson Lab experiment, E94101.
[18] T. Averett *et al.*, approved Jefferson Lab experiment E97103.
[19] C. Keppel *et al.*, approved Jefferson Lab experiment E94110.
[20] R.C. Walker *et al.*, Phys. Rev. D **49**, 5671 (1994).
[21] L. Andivahis *et al.*, Phys. Rev. D **50**, 5491 (1994).
[22] A. Bodek, Phys. Rev. D **20**, 1471 (1979).
[23] P. Stoler, Phys. Rev. D **44**, 73 (1991); Phys. Rev. Lett. **66**, 1003 (1991).
[24] L. Stuart *et al.*, Phys. Rev. D **58**, 032003 (1998).
[25] F.E. Close, *An Introduction to Quarks and Partons* (Academic, New York, 1979).
[26] Particle Data Group, C. Caso *et al.*, Eur. Phys. J. C **3**, 1 (1998).
[27] E.D. Bloom *et al.*, Phys. Rev. Lett. **23**, 930 (1969).
[28] V.V. Frolov, Ph.D. thesis, Rensselaer Polytechnic Institute, 1998.
[29] C.S. Armstrong, Ph.D. thesis, College of William and Mary, 1998.
[30] CTEQ Collaboration, H.L. Lai *et al.*, Phys. Rev. D **55**, 1280 (1997).
[31] A.D. Martin, R.G. Roberts, and W.J. Stirling, Phys. Rev. D **50**, 6734 (1994).
[32] New Moon Collaboration, M. Arneodo *et al.*, Phys. Lett. B **364**, 107 (1995). M. Arneodo *et al.*, Report No. CERN-PPE/95-138.
[33] W.R. Frazer and J.F. Gunion, Phys. Rev. Lett. **45**, 1138 (1980).
[34] S. Liuti (in preparation).
[35] O. Nachtmann, Nucl. Phys. **B63**, 237 (1973).
[36] J. L. Miramontes *et al.*, Z. Phys. C **41**, 247 (1988); Phys. Rev. D **40**, 2184 (1989).
[37] H. Georgi and Politzer, Phys. Rev. D **14**, 1829 (1976).
[38] K. Bitar, P.W. Johnson, and Wu-ki Tung, Phys. Lett. **83B**, 114 (1979).
[39] L.F. Abbott, W.B. Atwood, and R.M. Barnett, Phys. Rev. D **22**, 582 (1980).
[40] D.W. Duke and R.G. Roberts, Phys. Lett. **94B**, 417 (1980).
[41] M.R. Pennington and G.G. Ross, Nucl. Phys. **B179**, 324 (1981).
[42] M. Gari and W. Krümpelmann, Z. Phys. A **322**, 689 (1985).
[43] C. Keppel, S. Liuti, and I. Niculescu (in preparation).
[44] S. Gottlieb, Nucl. Phys. **B139**, 125 (1978).
[45] C.D. Cothran, D.B. Day, and S. Liuti, Phys. Lett. B **421**, 46 (1998).
[46] WA59 Collaboration, K. Varvell *et al.*, Z. Phys. C **36**, 1 (1987).